

Joint Answering and Explanation for Visual Commonsense Reasoning

Zhenyang Li, Yangyang Guo, Kejie Wang, Yinwei Wei, *Member, IEEE*, Liqiang Nie, *Senior Member, IEEE*, Mohan Kankanhalli, *Fellow, IEEE*

Abstract—Visual Commonsense Reasoning (VCR), deemed as one challenging extension of the Visual Question Answering (VQA), endeavors to pursue a more high-level visual comprehension. It is composed of two indispensable processes: question answering over a given image and rationale inference for answer explanation. Over the years, a variety of methods tackling VCR have advanced the performance on the benchmark dataset. Despite significant as these methods are, they often treat the two processes in a separate manner and hence decompose the VCR into two irrelevant VQA instances. As a result, the pivotal connection between question answering and rationale inference is interrupted, rendering existing efforts less faithful on visual reasoning. To empirically study this issue, we perform some in-depth explorations in terms of both language shortcuts and generalization capability to verify the pitfalls of this treatment. Based on our findings, in this paper, we present a plug-and-play knowledge distillation enhanced framework to couple the question answering and rationale inference processes. The key contribution is the introduction of a novel branch, which serves as the bridge to conduct processes connecting. Given that our framework is model-agnostic, we apply it to the existing popular baselines and validate its effectiveness on the benchmark dataset. As detailed in the experimental results, when equipped with our framework, these baselines achieve consistent and significant performance improvements, demonstrating the viability of processes coupling, as well as the superiority of the proposed framework.

Index Terms—Visual Commonsense Reasoning, Language Shortcut, Knowledge Distillation.

I. INTRODUCTION

VISUAL Question Answering (VQA) is to answer a natural language question pertaining to a given image [1], [2]. Despite its noticeable progress, existing VQA benchmarks merely address the simple recognition questions (e.g., *how many* or *what color*), while neglecting the explanation of the answer prediction. In the light of this, the task of Visual Commonsense Reasoning (VCR) [3] has recently been introduced to bridge this gap. Beyond answering the cognition-level questions ($Q \rightarrow A$) as canonical VQA does, VCR further prompts to yield a rationale for the right answer ($QA \rightarrow R$), as shown in Figure 1.

In fact, VCR is more challenging than VQA mainly due to the following two aspects: 1) On the data side - The images in the VCR dataset describe more sophisticated scenes (e.g., social interactions or mental states). Therefore, the related questions are rather difficult which often demand high-level

Zhenyang Li, Kejie Wang and Liqiang Nie are with Shandong University, China. E-mail: {zhenyanglidz, kjwang.henry, nieliqiang}@gmail.com.

Yangyang Guo, Yinwei Wei and Mohan Kankanhalli are with National University of Singapore, Singapore. E-mail: guoyang.eric@gmail.com, weiyinwei@hotmail.com, mohan@comp.nus.edu.sg.

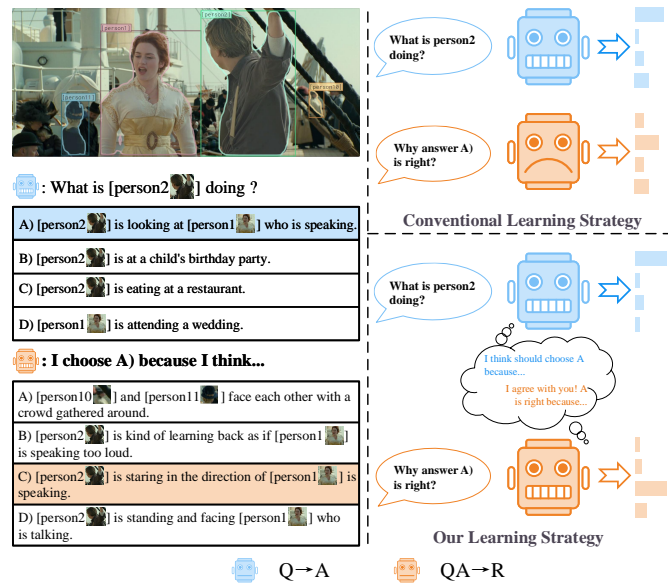


Fig. 1. Visual comparison between ours and conventional learning strategies. Different from previous methods separately treating $Q \rightarrow A$ and $QA \rightarrow R$, ours in the bottom, couple these two processes together by their non-separable nature.

visual reasoning capabilities (e.g., *why* or *how*). And 2) on the task side - It is hard to holistically produce both the right answer and rationale. VCR models should first predict the right answer, based on which the acceptable rationale can be further inferred from a few candidates. As question answering about the complex scenes has been proved non-trivial, locating the right rationale simultaneously in VCR thus leads to more difficulties.

To address the aforementioned research challenges, several prior efforts have been dedicated to VCR ever since its emergence. The initial attempts contribute to designing specific architectures to cope with this challenging task, such as R2C [3] and CCN [4]. In addition, recent BERT-based pre-training approaches, such as ViLBERT [5] and ERNIE-ViL [6], are recognized as the optimal solution to the first challenge. Specifically, a *pretrain-then-finetune* learning scheme is adopted to transfer knowledge from other multi-modal large-scale datasets to VCR. These methods, though keep advancing the boundaries of the benchmark, all consider $Q \rightarrow A$ and $QA \rightarrow R$ as two independent processes. As a result, the question answering and rationale inference processes are hard to holistically resolved. Namely, the second challenge still remains unsettled in literature.

Separately treating $Q \rightarrow A$ and $QA \rightarrow R$ brings adverse effects for visual reasoning, considering that these two processes share consistent goal by nature. On the one hand, $Q \rightarrow A$ provides the reasoning clues for $QA \rightarrow R$ to infer the right rationale. On the other hand, $QA \rightarrow R$ offers the explanation for $Q \rightarrow A$ to justify why the predicted answer is correct. Nevertheless, separately treating these two processes leads VCR to degenerate into two independent VQA tasks¹, resulting in the following two key defects: 1) Without direct guidance from $Q \rightarrow A$, $QA \rightarrow R$ has to rely on other unexpected information (e.g. word overlaps between answers and rationales), rendering the explanation less meaningful. And 2) since the two processes are mutually black boxes to each other, the process learning often overfits the in-domain data, which severely degrades the model robustness on out-of-domain. In this work, we perform an in-depth analysis about the defects mentioned above (ref. Section III).

By conforming to the task intuition and human cognition, the answering ($Q \rightarrow A$) and reasoning ($QA \rightarrow R$) should be made cohesive and consistent rather than separate. To this end, we propose a novel plug-and-play knowledge distillation enhanced framework to perform Answering and Reasoning Coupling (ARC for short). The key to our framework is the introduction of another proxy process - $QR \rightarrow A$. It takes as inputs the given question and the right rationale, and endeavors to perform answer prediction. In a sense, $QR \rightarrow A$ shares the same goal with $Q \rightarrow A$ yet is more information rich in input, and its reasoning procedure should be similar with $QA \rightarrow R$ as these two are actually complementary to each other. In particular, we devise two novel Knowledge Distillation (KD) modules: KD-A and KD-R. The former aligns the predicted logits between $Q \rightarrow A$ and $QR \rightarrow A$, since the answering with right rationale is expected to be more confident. While the latter, which is pivotal to maintain semantic consistency between $QA \rightarrow R$ and $QR \rightarrow A$, aligns the fused multi-modal features between these two. With the aid of the above two KD modules, the baselines are enabled to couple the answering and reasoning together, such that the visual reasoning is made more effective.

In summary, the contribution of this paper is three-fold:

- We revisit VCR from the perspective of coupling the $Q \rightarrow A$ and $QA \rightarrow R$ processes. With extensive probing tests, we find that separately treating the two processes, as adopted by existing VCR methods, is detrimental to visual reasoning, highlighting the necessity of coupling the answering and reasoning processes. To the best of our knowledge, this work is among the first efforts to jointly explore the two processes in VCR.
- We propose a novel plug-and-play knowledge distillation enhanced framework. Our newly introduced $QR \rightarrow A$ branch, serves as a proxy to couple $Q \rightarrow A$ and $QA \rightarrow R$.
- We apply this framework on several baseline methods and conduct experiments on the VCR benchmark dataset. The experimental results evidently demonstrate both the effectiveness and generalization capability of the proposed

method. The code has been released to facilitate other researchers².

The rest of this paper is structured as follows. We briefly review the related literature in Section II, and then discuss the pitfalls of existing methods in Section III, followed by our proposed ARC framework in Section IV. Experimental setup and result analyses are presented in Section V and Section VI, respectively. We finally conclude our work and outline the future work in Section VII.

II. RELATED WORK

A. Explanation in Visual Question Answering

Traditional VQA models mostly adopt a CNN-RNN learning paradigm, wherein the images are ingested via a pre-trained CNN network, in parallel to a RNN network taking the questions as input [1], [7], [8]. Many efforts have been devoted to applying the attention mechanism [9], [10], modular structure [11], [12] or external knowledge [13], [14] to VQA models. Until recently, some researchers have recognized the unfaithfulness of existing VQA models. For example, [15]–[17] aim to identify and overcome the language prior problem, i.e., the answers are blindly predicted based on certain short-cuts between questions and answers. Some methods instead, present to perform explanation for VQA models [18], [19]. For instance, some visual explanation approaches often harness the heat map to achieve *where to look*, such as Gram-CAM [20] or U-CAM [21]. VQA-HAT [22] collects human attention data which are utilized to supervise the visual attention learning. HINT [15] encourages VQA models to be sensitive to the same input regions as humans. Different from these approaches, VQA-E [18] requires a VQA model to generate a textual explanation for the answer prediction. Moreover, some multi-modal approaches that integrate both the visual and textual explanations provide the advantages of both to build more faithful VQA systems [23], [24].

B. Visual Commonsense Reasoning

VCR contributes to an indispensable branch to the explainable VQA [3]. It involves two processes: question answering ($Q \rightarrow A$) and rationale inference ($QA \rightarrow R$). Both are embodied in a multiple-choice fashion. VCR forces an approach to not only answer the given question, but also provide a reasonable explanation to the $Q \rightarrow A$ process. It thus makes the answer prediction more transparent and user-friendly to humans.

Existing studies are in fact very sparse due to its challenging nature. Some of them resort to designing specific model architectures [3], [4], [25], [26]. For instance, R2C [3] adopts a three-step way to tackle this task, *grounding* texts with respect to the involved objects; *contextualizing* the answer with the corresponding question and objects; and finally *reasoning* over the shared representation. Inspired by the neuron connectivity of brains, CCN [4] dynamically models the visual neuron connectivity, which is contextualized by the queries and responses. HGL [25] leverages a vision-to-answer and a dual question-to-answer heterogeneous graphs to seamlessly bridge vision and

¹Note that for $QA \rightarrow R$, the *query* to a VQA model now becomes the concatenation of the original question and the right answer. And the corresponding *answer* choices are the set of candidate rationales.

²<https://github.com/SDLZY/ARC>.

language. Recently, BERT-based pre-training approaches have been extensively explored in the vision-and-language domain. In general, most of them employ a *pretrain-then-transfer* scheme and achieve significant performance improvement on VQA benchmarks including VCR [5], [27], [28]. These models are often firstly pre-trained on large-scale multi-modal datasets (such as Conceptual Captions [29]), which is then followed by the fine-tuning procedure on VCR.

However, one limitation still prevents these methods from further advancement, namely, the $Q \rightarrow A$ and $QA \rightarrow R$ processes are consumed independently. Such an approach makes the answer prediction and rationale inference as two independent VQA tasks. In this work, we propose to address this issue through combining these two processes.

C. Knowledge Distillation

The past few years have witnessed the noticeable development of KD [30], [31]. As an efficacious model compression tool, KD is able to transfer the knowledge from a cumbersome network (teacher network) to a more compact one (student network). Based on its application scope, previous KD methods can be roughly categorized into two groups - logits-based and feature-based. The logits-based methods [30], [32] encourage the student to imitate the output from a teacher model. For example, the vanilla KD utilizes the softened logits from a pretrained teacher network as an extra supervision to instruct the student [30]. In contrast, feature-based methods [31], [33], [34] attempt to transfer the knowledge in intermediate features between the two networks. FitNet [35] directly matches the embeddings of each example between the teacher and student networks. Attention Transfer [36] extends FitNet from embedding to attention matching for different levels of feature maps. To reduce the performance gap between the teacher and student, RCO [37] presents route constrained hint learning, supervising the student by the outputs of hint layers from the teacher. Besides, FSP [38] estimates the Gram matrix across layers to reflect the data flow of how the teacher network learns.

III. PITFALL OF EXISTING VCR METHODS

The task of Visual Commonsense Reasoning is challenging in the sense that the model is required to not only answer a question, but also correctly reason about the answer prediction. Consequently, the two processes are complementary and inseparable to each other. However, as mentioned earlier, existing methods treat $Q \rightarrow A$ and $QA \rightarrow R$ separately, breaking the bridge between these two. In view of this, we explore the negative effects of this treatment from the following two aspects.

A. Language Shortcut Recognition

Existing methods all employ an independent model for $QA \rightarrow R$, and achieve improved performance. This motivates us to question: what kinds of clues do these methods employ, excluding the $Q \rightarrow A$ reasoning information? To address this question, we firstly recognize that the overlapped words

between right answers and rationales dominate the rationale prediction. For instance, in Figure 1, the correct rationale largely overlaps with the right answer, e.g., the ‘[person1]’ and ‘[person2]’ tag and the word ‘speaking’. This may lead the models to predict rationale based on these shortcuts rather than performing visual explanation for $Q \rightarrow A$. The evidence is elaborated as follows.

A \rightarrow R Accuracy Calculation. We input only the correct answer as the query to predict rationales with other settings untouched, and show the results in Table I. It can be observed that the three models only degrade slightly when removing the question input. As VCR is a question-driven task, it can be expected that the visual reasoning becomes meaningless without the questions. Nevertheless, the answer-only variants of these methods also achieve very competitive results, contradicting our expectations.

TABLE I
RATIONALE PREDICTION PERFORMANCE COMPARISON WITH AND WITHOUT THE QUESTION.

Model	$QA \rightarrow R$	$A \rightarrow R$
R2C [3]	67.2	66.3
HGL [25]	70.6	69.8
CCN [4]	70.5	70.4

Attention Distribution over Queries. As the attention module plays an essential part in current VCR models, we further explore the shortcut visually from the perspective of attention. For this experiment, we consider only the $QA \rightarrow R$. Given the attention map $\mathbf{W} \in \mathbb{R}^{(l_q+l_a) \times l_r}$ for a query-rationale³ pair, where l_q , l_a and l_r respectively denote the length of question, answer and rationale, we use the following formula to estimate the attention contribution from the answer side:

$$ratio_{ans} = \frac{\sum_{i=l_q+1}^{l_q+l_a} \sum_{j=1}^{l_r} \mathbf{W}_{[i,j]}}{\sum_{i=1}^{l_q+l_a} \sum_{j=1}^{l_r} \mathbf{W}_{[i,j]}} \quad (1)$$

where $\mathbf{W}_{[i,j]} \in \mathbf{W}$ is the attention score between the query token q_i and the rationale token r_j . Thereafter, we find that the median of $ratio_{ans}$ in three methods (HGL, R2C and CCN) on the validation set is 0.72, 0.78, and 0.86 respectively, indicating that the current models pay more attention to the answer side. Two instances produced from R2C are illustrated in Figure 2. From this figure, we can conclude that current methods mainly rely on the answer information to yield the right rationale, while the questions are somewhat ignored.

B. Generalization on Skewed Data

We now explore the generalization capability of existing methods over the out-of-domain data. To this end, we rewrite some sentences (including questions, answers and rationales) while maintaining their semantic meanings. The Paraphrase-Online tool⁴ is leveraged to implement this, where we simply

³The query is the original question appended with the right answer.

⁴<https://www.paraphrase-online.com/>.

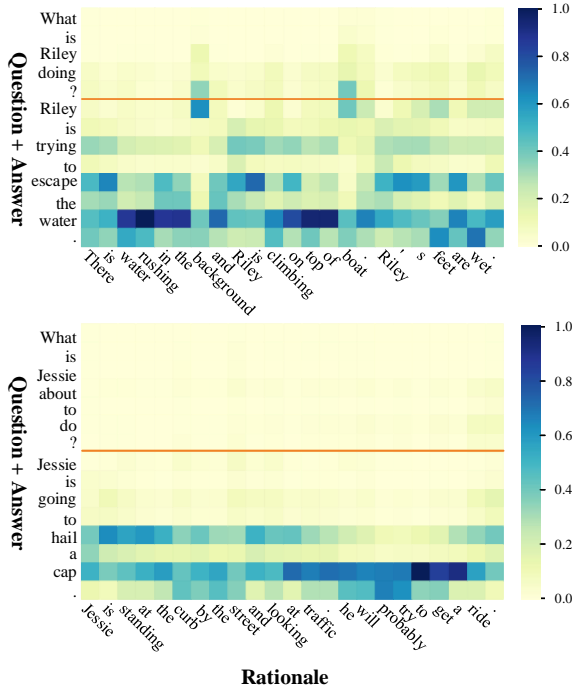


Fig. 2. Illustration of the attention distribution of QA→R from R2C. The orange line splits the question and answer from queries.

TABLE II
A REWRITTEN EXAMPLE FROM OUR EXPERIMENTS.

Original	Paraphrased
What is [person4] getting ready to do?	What is [person4] getting prepared to do?
He's about to start singing.	He's around to begin singing.
Everyone else is singing and he seems to be getting ready to follow suit.	Everyone else is singing and he appears to be getting prepared to copy them.

substitute some verbs/nouns with their synonyms. Some examples are illustrated in Table II. In the next step, we apply the above methods on the rewritten data and evaluate their performance. From Table III, we find that all models degrade drastically on these data, implying that they largely overfit on the in-domain data and lack generalization ability.

TABLE III
QA→R PERFORMANCE COMPARISON OVER TWO VERSIONS OF THE VALIDATION SET. *Original* AND *Paraphrased* MEAN THE MODELS ARE TESTED ON ORIGINAL AND REWRITTEN VCR VALIDATION SET, RESPECTIVELY.

Model	Q→A		QA→R	
	Original	Paraphrased	Original	Paraphrased
R2C [3]	63.8	52.6	67.2	54.7
CCN [4]	66.8	54.7	70.6	56.5
TAB-VCR [26]	69.9	56.4	72.2	60.5

Based on the above two findings, we notice that the current models fail to conduct visual reasoning based on the answering clues. They instead leverage superficial correlations or simply

overfit on the in-domain data. To solve this problem, a VCR model is expected to benefit from answering and reasoning jointly.

IV. METHOD

The above probing tests demonstrate that separately treating the two processes in VCR leads to unsatisfactory outcomes. To overcome this, we propose the ARC framework to couple Q→A and QA→R together. In fact, directly coupling these two is rather difficult, as there exists a strong textual shortcut between right answers and rationales. We instead, introduce another new branch, namely QR→A, as a bridge to achieve this goal.

A. Preliminary

Before delving into the details of our ARC, we first outline the three processes involved in our framework, and their corresponding learning functions.

1) *Process Definition*: Our framework contains three processes: two of them are formally defined by the original VCR (i.e., Q→A and QA→R) and the other is a new process defined by us (QR→A). Note that all the three processes are formulated in a multiple choice format. That is, given an image I and a *query* related to the image, the model is required to select the right choice from *candidate responses*.

Q→A: Its query is embodied with a question Q , and the candidate responses are a set of answer choices \mathcal{A} . The objective is to select the right answer A :

$$A = \operatorname{argmax}_{A_i \in \mathcal{A}} f^A(Q, I, A_i), \quad (2)$$

where f^A denotes the Q→A model.

QA→R: The query is the concatenation of the question Q and the right answer A . A set of rationales \mathcal{R} constitute the candidate responses and the model is expected to choose the right rationale R :

$$R = \operatorname{argmax}_{R_i \in \mathcal{R}} f^R(Q, A, I, R_i), \quad (3)$$

where f^R denotes the QA→R model.

One can see that it is difficult to directly connect these two since the involved parameters are not shared and the input to QA→R includes the ground-truth answer rather than the predicted one. In view of this, to bridge these two, we introduce the QR→A as a proxy.

QR→A: The query and responses are respectively the concatenation of the question Q along with the right rationale R and answer choices. The objective is:

$$A = \operatorname{argmax}_{A_i \in \mathcal{A}} f^C(Q, R, I, A_i), \quad (4)$$

where f^C denotes the QR→A model. On the one hand, QR→A shares the consistent objective with Q→A. On the other hand, its reasoning should be similar to that of QA→R. These two factors make QR→A a good proxy for connecting Q→A and QA→R.

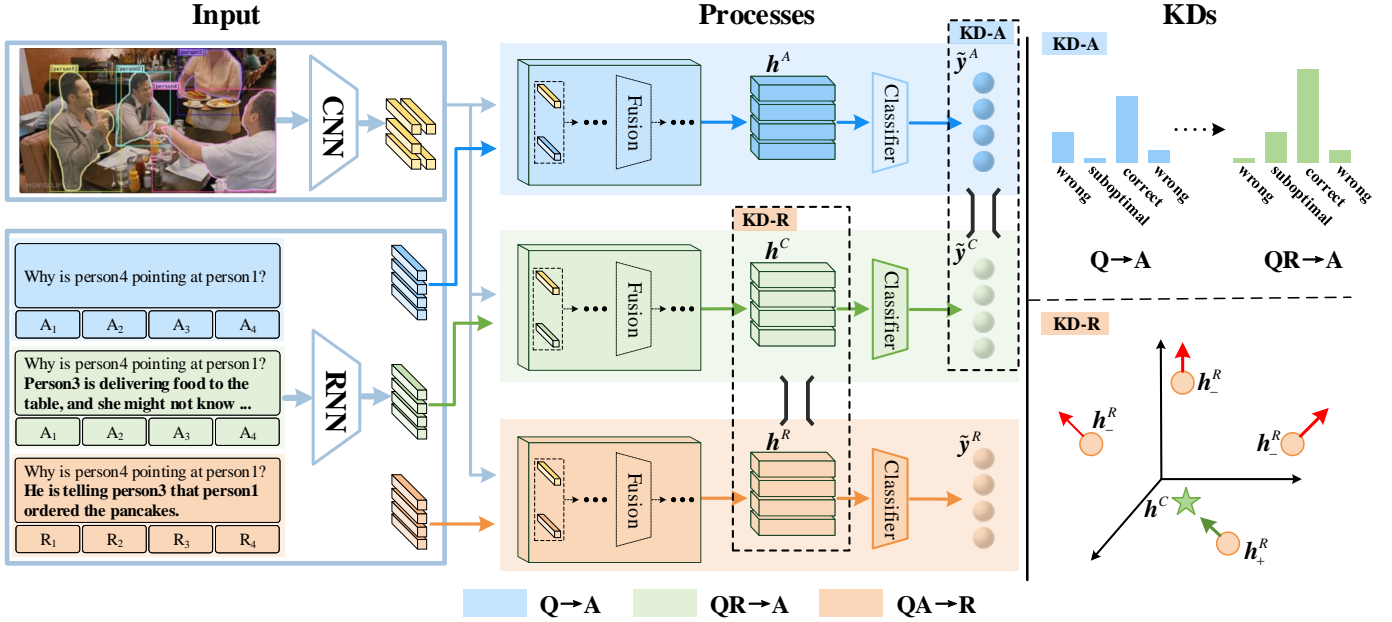


Fig. 3. The overall architecture of our framework. There are three processes, i.e., $Q \rightarrow A$, $QR \rightarrow A$ and $QA \rightarrow R$. We then bridge these processes with two novel KD modules: KD-A is leveraged to align the predicted logits between $QR \rightarrow A$ and $Q \rightarrow A$; and KD-R aims to maintain semantic consistency between $QR \rightarrow A$ and $QA \rightarrow R$ via the feature-level knowledge distillation.

2) *Training Pipeline*: In general, for the feature extractors, the VCR model often uses a pre-trained CNN network to obtain the visual features from the input image I , and an RNN-based or Transformer-based network to extract the textual features of the query and response. Thereafter, a multi-modal fusion module is employed to obtain the joint representation, followed by the classifier to predict the logit \tilde{y}_i for the response i .

To achieve the objectives in Equation 2 and 3, previous methods often separately optimize the following two cross-entropy losses,

$$\mathcal{L}^A = - \sum_i^{|A|} y_i^A \log \frac{\exp \tilde{y}_i^A}{\sum_j \exp \tilde{y}_j^A}, \quad (5)$$

$$\mathcal{L}^R = - \sum_i^{|R|} y_i^R \log \frac{\exp \tilde{y}_i^R}{\sum_j \exp \tilde{y}_j^R}, \quad (6)$$

where y_i^A and y_i^R denote the ground truth label of answer A_i and rationale R_i , respectively.

In all the existing VCR methods, the models f^A and f^R share the identical architecture and are trained separately. In other words, the two processes are reduced into two independent VQA tasks, resulting in lacking the connection between answering and reasoning. In the next, we present our model-agnostic framework to couple the two successive processes, i.e., $Q \rightarrow A$ and $QA \rightarrow R$, together.

B. Proposed Method

In order to effectively integrate the above three processes, we propose a dual-level knowledge distillation framework, and illustrate it in Figure 3. Specifically, after extracting the fused multi-modal features with the aforementioned backbones, we

further develop two parallel knowledge distillation modules to bridge the $QR \rightarrow A$ with other two processes. Our first KD module is leveraged to align the predicted scores from $QR \rightarrow A$ and $Q \rightarrow A$. The two processes share the same objective and $QR \rightarrow A$ offers ample information for picking the right answer. In this way, we take the predictions from $QR \rightarrow A$ as the teacher and the predictions from $Q \rightarrow A$ as the student. Our second KD module is required to align the feature learning between $QR \rightarrow A$ and $QA \rightarrow R$. Despite the objectives being distinct, the reasoning of these two is actually similar. That is, answering with the given right rationale is simply the reverse of reasoning given the right answer, which allows these two processes to share related features. As can be evidently observed from Figure 3, these two KDs provide two bridges to connect $Q \rightarrow A$ and $QA \rightarrow R$.

1) *Knowledge Distillation between $QR \rightarrow A$ and $Q \rightarrow A$ (KD-A)*: Since the rationale is yielded for explaining the right answer, we incorporate the correct rationale with the given question for answer prediction. It is intuitive that when combined with the correct rationale, the answering confidence should be increased. In the light of this, we simply take the output scores from $QR \rightarrow A$ as the teacher, and make them guide the learning of $Q \rightarrow A$.

Specifically, in this KD module, the knowledge is encoded and transferred in the form of softened scores: it aligns the output probability p^A (from the student f^A) with the p^C (from the teacher f^C). As it is noted that p^C might be close to the one-hot encoding of the ground-truth label, a relaxation temperature $T > 1$ is introduced to soften the logits \tilde{y}^C from f^C , and thus, provide more information during training. The same relaxation is applied to the output logits \tilde{y}^A of f^A :

$$p_i^C = \frac{\exp(\tilde{y}_i^C/T)}{\sum_{j=1}^{|A|} \exp(\tilde{y}_j^C/T)}, \quad (7)$$

$$p_i^A = \frac{\exp(\tilde{y}_i^A/T)}{\sum_{j=1}^{|A|} \exp(\tilde{y}_j^A/T)}. \quad (8)$$

We then use the KL divergence to align the predicted scores as follows,

$$\mathcal{L}_{KD}^A = D_{KL}(\mathbf{p}^C || \mathbf{p}^A). \quad (9)$$

2) *Knowledge Distillation between QR→A and QA→R (KD-R)*: We argue that the features learned by QR→A are more reliable than that of QA→R. The support for this comes from two sides: QR→A resembles to *raising questions with right answers*, providing explicit evidence for feature learning; leveraging QA→R to perform reasoning might lead to textual shortcut problem, as discussed in Section III-A.

To this end, we design another knowledge distillation module to align the feature learning between QR→A and QA→R, which maintains the semantic consistency. In particular, we firstly leverage the multi-modal fused feature \mathbf{h}^C from the $f^C(Q, R, I, A_{gt})$ as the teacher feature, where the answer input A_{gt} denotes the ground-truth one. As for the fused features $\{\mathbf{h}_i^R\}_{i=1}^{|\mathcal{R}|}$ from f^R , one is from the right rationale while the others are from the remaining candidates. We denote the right one as \mathbf{h}_+^R and the false one as \mathbf{h}_-^R , and estimate the similarity score with the following formula,

$$s_i = \mathbf{h}^C \cdot \mathbf{h}_i^R, \quad (10)$$

where \cdot represents the dot product and s_i is the estimated score. In its optimal setting, s_+ should be larger than s_- . To enable its training, we adopt the rationale labels as supervision signal and perform KD-R with,

$$\mathcal{L}_{KD}^R = - \sum_i^{|\mathcal{R}|} y_i^R \log \frac{\exp s_i}{\sum_j^{|\mathcal{R}|} \exp s_j}. \quad (11)$$

C. Training Protocol

With the above two KD modules, we then combine them with the original answering and reasoning losses as follows:

$$\mathcal{L}_{Q \rightarrow A} = \alpha \mathcal{L}_{KD}^A + (1 - \alpha) \mathcal{L}^A, \quad (12)$$

$$\mathcal{L}_{QA \rightarrow R} = \beta \mathcal{L}_{KD}^R + (1 - \beta) \mathcal{L}^R, \quad (13)$$

where α and β are tunable parameters to balance the two knowledge distillation losses.

Finally, we train the entire framework in an end-to-end way:

$$\mathcal{L} = \mathcal{L}_{Q \rightarrow A} + \mathcal{L}_{QA \rightarrow R}. \quad (14)$$

Different from previous methods that output answers and rationales separately, in our framework, the answers and rationales are predicted by f^A and f^R at the same time, respectively. In this way, the Q→A and QA→R are made more cohesive than these methods.

The optimization procedure of our proposed ARC, as shown in Algorithm 1, contains two stages. On the first stage, we train the teacher network f^C until its cross-entropy loss converges (line 1-4),

$$\mathcal{L}^C = - \sum_i^{|A|} y_i^A \log \frac{\exp \tilde{y}_i^C}{\sum_j \exp \tilde{y}_j^C}, \quad (15)$$

where \tilde{y}_i^C denotes the output of f^C corresponding to answer A_i . Secondly, the f^A and f^R are updated together, where the cross-entropy losses and knowledge distillation losses are both considered (line 5-10). During testing, the f^C branch is removed, and only f^A and f^R predict answers and rationales simultaneously.

Algorithm 1 Training Procedure of ARC

Require: Training set \mathcal{D}^A , \mathcal{D}^R and \mathcal{D}^C for three processes respectively.

- 1: **for** each batch $\mathcal{B}^C \in \mathcal{D}^C$ **do**
 - 2: Estimate \mathcal{L}^C by Equation 15;
 - 3: Update f^C by \mathcal{L}^C ;
 - 4: **end for**
 - 5: **for** each batch $\mathcal{B}^A \in \mathcal{D}^A$ and $\mathcal{B}^R \in \mathcal{D}^R$ **do**
 - 6: Estimate $\mathcal{L}_{Q \rightarrow A}$ by Equation 12;
 - 7: Estimate $\mathcal{L}_{QA \rightarrow R}$ by Equation 13;
 - 8: Sum above losses by Equation 14;
 - 9: Update f^A and f^R ;
 - 10: **end for**
-

V. EXPERIMENTAL SETUP

A. Datasets and Evaluation Protocols

We conducted extensive experiments on the VCR [3] benchmark dataset. In specific, the images are extracted from the movie clips in LSMDC and MovieClips⁵, wherein the objects in images are detected by Mask-RCNN [39]. We utilized the official dataset split, where the number of instances for training, validation and test are 212,923, 26,534 and 25,263, respectively. For all the three processes, four options serve as candidates and only one is correct.

Regarding the evaluation metric, we adopted the popular accuracy metric for Q→A, QA→R and Q→AR. For Q→AR, the prediction is right only when both the answer and rationale are selected correctly. Since the testing set labels are not available, we reported the performance of our best model on the testing set once and performed other experiments on the validation set.

B. Implementation Details

The PyTorch toolkit is leveraged to implement our method and all the experiments were conducted on a single GeForce RTX 2080 Ti GPU. We strictly followed the baselines to utilize the ResNet-50 [40] and BERT [41] as our backbone and initialized all the trainable parameters. Unless otherwise noted, Adam with weight decay of 1e-4 and beta of 0.9 is adopted to optimize all model parameters. The initial learning rate is 2e-4, reducing half ($\times 0.5$) for two epochs when the validation accuracy is not increasing.

C. Baselines

We compared our method with the following two sets of baselines.

⁵youtube.com/user/movieclips.

TABLE IV
PERFORMANCE COMPARISON ON VCR VALIDATION AND TESTING SETS.

Model	$Q \rightarrow A$		$QA \rightarrow R$		$Q \rightarrow AR$		
	Val	Test	Val	Test	Val	Test	
Chance	25.0	25.0	25.0	25.0	6.2	6.2	
VQA	RevisitedVQA [42]	39.4	40.5	34.0	33.7	13.5	13.8
	BUTD [43]	42.8	44.1	25.1	25.1	10.7	11.0
	MLB [44]	45.5	46.2	36.1	36.8	17.0	17.2
	MUTAN [45]	44.4	45.5	32.0	32.2	14.6	14.6
VCR	R2C [3]	63.8	65.1	67.2	67.3	43.1	44.0
	CCN [4]	66.6	67.2	68.3	68.2	45.5	46.1
	TAB-VCR [26]	69.9	70.4	72.2	71.7	50.6	50.5
Ours	R2C+Ours	66.2	66.9	69.1	69.4	45.9	46.6
	CCN+Ours	69.0	70.0	71.1	70.6	49.3	49.7
	TAB-VCR+Ours	70.5	71.4	73.1	72.6	51.8	52.1
Human	-	91.0	-	93.0	-	85.0	

1) *VQA baselines*: RevisitedVQA [42], BottomUpTopDown [43], MLB [44] and MUTAN [45]. These methods are originally developed for VQA, and adapted for VCR in this paper.

2) *Methods specifically designed for VCR*: We employed our method to the following baselines to validate its effectiveness: R2C [3], CCN [4] and TAB-VCR [26]. The implementation details of these methods are the same as our ARC in Section V-B.

- **R2C** leverages ResNet [40] and BERT to extract visual and text features, respectively. Its multimodal fusion module contains two bilinear attention networks and one LSTM to perform contextualization and reasoning between the image and text.
- **CCN** extracts features in the same way as R2C, while uses a more complex connective cognition network for cognitive reasoning through dynamically reorganizing visual neuron connectivity in the fusion module.
- **TAB-VCR** improves visual features with the attribute information and accordingly associates more words in the text with the detected objects in the image for better image-text grounding.

VI. EXPERIMENTAL RESULTS

A. Overall Performance Comparison

The results on both validation and testing sets are reported in Table 1, and the key observations are listed as follows.

- For all the four VCR baselines, with our ARC framework, they can all achieve significant gains on both validation and test sets. For example, compared with CCN, 2.8%, 2.4% and 3.6% performance improvement on $Q \rightarrow A$, $QA \rightarrow R$ and $Q \rightarrow AR$ on the test set can be observed, respectively. It proves the necessity to couple the $Q \rightarrow A$ and $QA \rightarrow R$ as well as the effectiveness of the proposed method.
- Traditional state-of-the-art VQA methods all perform less favorable than the VCR ones. The reasons for this are two-fold: 1) the answers in previous VQA datasets are

TABLE V
ABLATION STUDY OF THE PROPOSED METHOD ON VCR VALIDATION SET. **KD-R** DENOTES THE KD BETWEEN $QR \rightarrow A$ AND $QA \rightarrow R$. **KD-A** REPRESENTS THE KD BETWEEN $QR \rightarrow A$ AND $Q \rightarrow A$.

Methods	$Q \rightarrow A$	$QA \rightarrow R$	$Q \rightarrow AR$	$QR \rightarrow A$
R2C	63.8	67.2	43.1	-
R2C+KD-R	65.3	68.7	45.1	-
R2C+KD-R+KD-A	66.2	69.1	45.9	92.6
CCN	66.6	68.3	45.5	-
CCN+KD-R	68.5	70.7	48.7	-
CCN+KD-R+KD-A	69.0	71.1	49.3	92.9
TAB-VCR	69.9	72.2	50.6	-
TAB-VCR+KD-R	70.1	72.8	51.3	-
TAB-VCR+KD-R+KD-A	70.5	73.1	51.8	93.1

composed of a few key words, while the answer length in VCR is relatively longer (7.5 words for answers and 16 words for rationales in average). And 2) VCR demands high-order reasoning capability, which is far beyond the simple recognition in VQA settings.

- The performance of VQA models on $Q \rightarrow A$ is worse than that of $QA \rightarrow R$, which is opposite to VCR methods. It is because that: 1) predicting the right rationale is more difficult for VQA models; 2) the specialized methods for VCR utilize the shortcuts between the right answer and rationales to improve prediction accuracy.

B. Ablation Study

We conducted detailed experiments to validate the effectiveness of each KD module and reported the results in Table V. From this table, we have the following observations:

- When incorporating the knowledge distillation module between $QR \rightarrow A$ and $QA \rightarrow R$ into the baseline model, a significant performance improvement can be observed. Take the R2C baseline as an example, our method boosts it by 1.5% ($Q \rightarrow A$), 1.5% ($QA \rightarrow R$) and 2.0% ($Q \rightarrow AR$). In addition, the $Q \rightarrow A$ model is also enhanced, partially due to the joint training of $Q \rightarrow A$ and $QA \rightarrow R$ from our proposed method.
- We then introduced the knowledge distillation module between $Q \rightarrow A$ and $QR \rightarrow A$ to the baseline model and observed further performance improvement. These two experiments validate the effectiveness of our knowledge distillation modules.
- All models demonstrate noticeably good results on $QR \rightarrow A$. This observation is intuitively correct and further verifies the advantage of making it as a proxy between $Q \rightarrow A$ and $QA \rightarrow R$.

C. Qualitative Results

We illustrate several cases qualitatively from the R2C baseline and our method in Figure 4. In detail, for the first example, although R2C gives the right answer, it fails to select the right rationale. It is because that the rationale option B contains more overlaps with the query (e.g., ‘[person1]’, ‘attractive’),

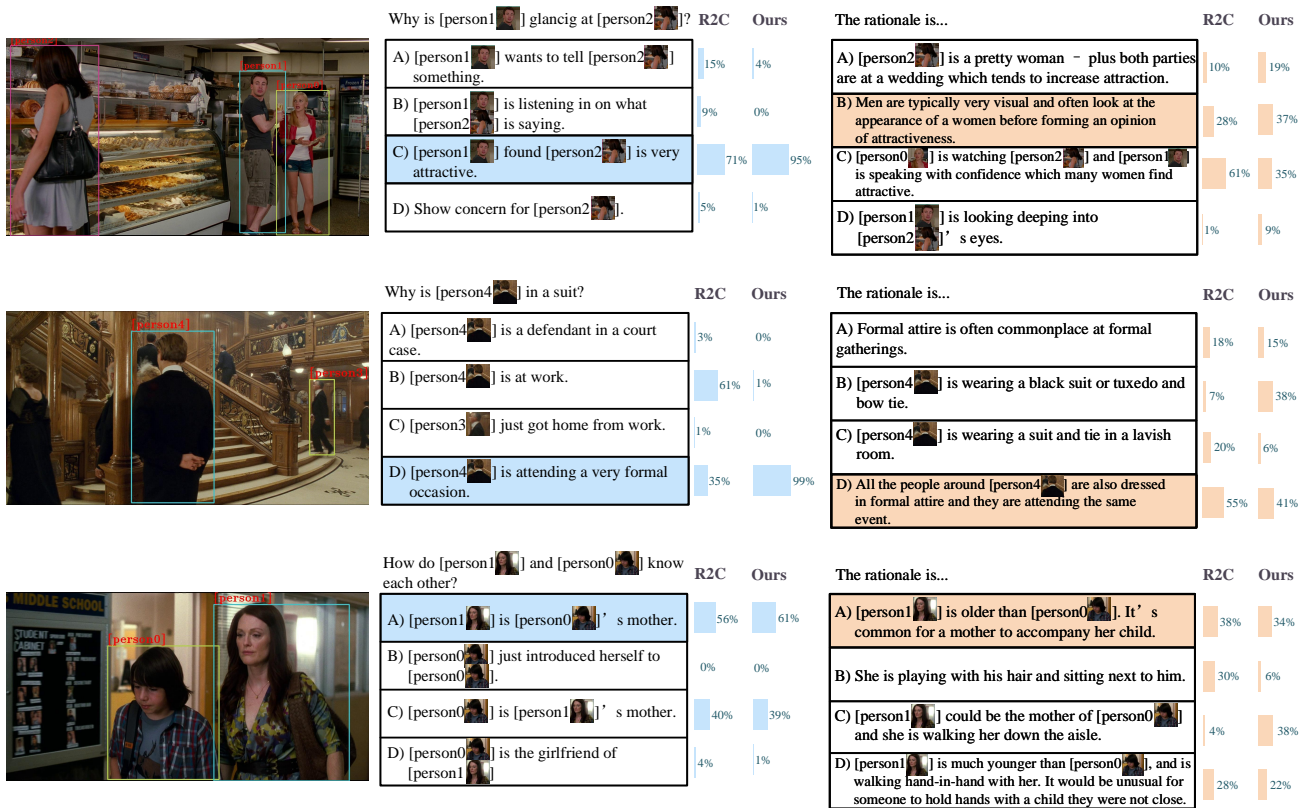


Fig. 4. Qualitative results from R2C and our method. The predicted score distribution is illustrated on the rightmost of each sample.

and R2C leverages such shortcut to perform reasoning. While with our method, the right rationale can be more confidently selected. The second example is even more confusing, as R2C reasons correctly, while the answer is not right. It is mainly because R2C makes answering and reasoning into two independent VQA instances. The last row demonstrates a failure case, where our model chooses the right answer but predicts the wrong rationale. The rationale chosen by our framework is also an explanation for the right answer although slightly deviates from the ground truth.

In addition, we also illustrate two instances with attention weight distribution in Figure 5. From this figure, we observe that our framework guides the baseline to focus more on the question part, such as ‘explosion’ in the first example, and ‘boss’ in the second example, and therefore reduce the language shortcut reliance.

D. Performance Improvement on Skewed Data

As previously shown in Table III, all existing models perform much less favorably on the skewed data. To examine whether coupling answering and reasoning could improve the generalization of these models, we applied our method on these data and reported the results in Table VI. With our proposed ARC, all the models obtain certain improvements. For instance, our method gains a 3.6%, 2.5% and 3.3% absolute improvement over R2C on the three accuracy metrics, respectively. It is evident that our method demonstrates strong generalization capability on these skewed data, and is affected less by the language shortcut compared with baselines.

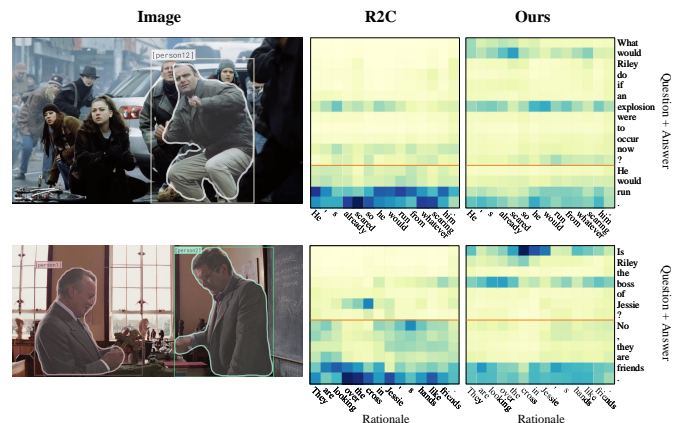


Fig. 5. Illustration of attention distribution from QA→R of baselines and ours.

E. Results w.r.t Question Types

As shown in Figure 6, we illustrate the question types defined by the corresponding matching words in the validation set and display the performance of R2C and our method with respect to the question types. In a nutshell, our method achieves consistent improvements on almost all question types. In particular, compared with binary questions like *is* and *do*, our method shows more advantage on the more challenging *where*, *how* and *what* questions. However, both methods struggle on the *how* questions, as these questions demand high-level visual understanding and are currently extremely difficult

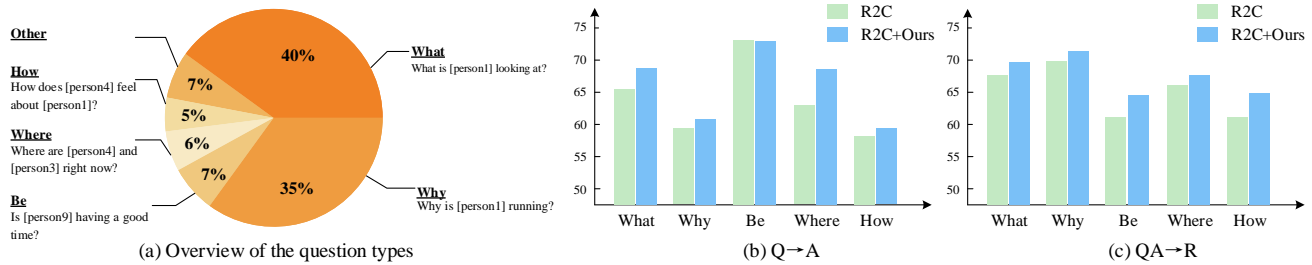


Fig. 6. Overview of question types in the VCR dataset (a) and performance comparison of Q→A (b) and QA→R (c).

TABLE VI
PERFORMANCE COMPARISON ON SKEWED DATA.

Methods	Q→A	QA→R	Q→AR
R2C [3]	52.8	54.7	29.3
R2C+Ours	56.4	57.2	32.6
CCN [4]	52.6	56.5	30.4
CCN+Ours	55.5	57.2	32.6
TAB-VCR [26]	56.4	60.5	34.9
TAB-VCR+Ours	57.8	61.3	36.0

to address.

VII. CONCLUSION AND FUTURE WORK

Existing VCR models perform the answering and explaining processes in a separate manner, leading to poor generalization and undesirable language shortcuts between answers and rationales. This paper firstly discusses the disadvantage of the separate training strategy, followed by a novel knowledge distillation framework to couple the two processes in VCR. Our framework consists of two KD modules, KD-A and KD-R, where the former is leveraged to align the predicted logits between Q→A and QR→A, and the latter aims to maintain semantic consistency between QA→R and QR→A with feature-level knowledge distillation. We applied this framework to several state-of-the-art baselines and studied its effectiveness on the VCR benchmark dataset. With the quantitative and qualitative experimental results, the viability of coupling the Q→A and QR→A is explicitly testified.

Regarding the future work, since this work demonstrates the potential of process coupling for enhancing visual understanding, exploring approaches from other model components, such as the attention module, is thus seemingly promising.

REFERENCES

- [1] S. Antol, A. Agrawal, J. Lu, M. Mitchell, D. Batra, C. L. Zitnick, and D. Parikh, "Vqa: Visual question answering," in *ICCV*, pp. 2425–2433, 2015.
- [2] Y. Zhu, O. Groth, M. Bernstein, and L. Fei-Fei, "Visual7w: Grounded question answering in images," in *CVPR*, pp. 4995–5004, 2016.
- [3] R. Zellers, Y. Bisk, A. Farhadi, and Y. Choi, "From recognition to cognition: Visual commonsense reasoning," in *CVPR*, pp. 6720–6731, 2019.
- [4] A. Wu, L. Zhu, Y. Han, and Y. Yang, "Connective cognition network for directional visual commonsense reasoning," in *NeurIPS*, pp. 5670–5680, 2019.
- [5] J. Lu, D. Batra, D. Parikh, and S. Lee, "Vilbert: Pretraining task-agnostic visiolinguistic representations for vision-and-language tasks," in *NeurIPS*, pp. 13–23, 2019.
- [6] F. Yu, J. Tang, W. Yin, Y. Sun, H. Tian, H. Wu, and H. Wang, "Ernie-vil: Knowledge enhanced vision-language representations through scene graphs," in *AAAI*, pp. 3208–3216, 2021.
- [7] M. Malinowski, M. Rohrbach, and M. Fritz, "Ask your neurons: A neural-based approach to answering questions about images," in *ICCV*, pp. 1–9, 2015.
- [8] Q. Wu, D. Teney, P. Wang, C. Shen, A. Dick, and A. van den Hengel, "Visual question answering: A survey of methods and datasets," *CVIU*, vol. 163, pp. 21–40, 2017.
- [9] P. Anderson, X. He, C. Buehler, D. Teney, M. Johnson, S. Gould, and L. Zhang, "Bottom-up and top-down attention for image captioning and visual question answering," in *CVPR*, pp. 6077–6086, 2018.
- [10] W. Guo, Y. Zhang, J. Yang, and X. Yuan, "Re-attention for visual question answering," *IEEE T-IP*, vol. 30, pp. 6730–6743, 2021.
- [11] J. Andreas, M. Rohrbach, T. Darrell, and D. Klein, "Neural module networks," in *CVPR*, pp. 39–48, 2016.
- [12] J. Johnson, B. Hariharan, L. Van Der Maaten, L. Fei-Fei, C. Lawrence Zitnick, and R. Girshick, "Clevr: A diagnostic dataset for compositional language and elementary visual reasoning," in *CVPR*, pp. 2901–2910, 2017.
- [13] P. Wang, Q. Wu, C. Shen, A. Dick, and A. Van Den Hengel, "Fvqa: Fact-based visual question answering," *IEEE T-PAMI*, vol. 40, no. 10, pp. 2413–2427, 2017.
- [14] K. Marino, M. Rastegari, A. Farhadi, and R. Mottaghi, "Ok-vqa: A visual question answering benchmark requiring external knowledge," in *CVPR*, pp. 3195–3204, 2019.
- [15] R. R. Selvaraju, S. Lee, Y. Shen, H. Jin, S. Ghosh, L. Heck, D. Batra, and D. Parikh, "Taking a hint: Leveraging explanations to make vision and language models more grounded," in *ICCV*, pp. 2591–2600, 2019.
- [16] Y. Guo, L. Nie, Z. Cheng, F. Ji, J. Zhang, and A. Del Bimbo, "Adavqa: Overcoming language priors with adapted margin cosine loss," in *IJCAI*, pp. 708–714, 2021.
- [17] A. Agrawal, D. Batra, D. Parikh, and A. Kembhavi, "Don't just assume; look and answer: Overcoming priors for visual question answering," in *CVPR*, pp. 4971–4980, 2018.
- [18] Q. Li, Q. Tao, S. Joty, J. Cai, and J. Luo, "Vqa-e: Explaining, elaborating, and enhancing your answers for visual questions," in *ECCV*, pp. 552–567, 2018.
- [19] B. Patro, V. Nambodiri, *et al.*, "Explanation vs attention: A two-player game to obtain attention for vqa," in *AAAI*, pp. 11848–11855, 2020.
- [20] R. R. Selvaraju, M. Cogswell, A. Das, R. Vedantam, D. Parikh, and D. Batra, "Grad-cam: Visual explanations from deep networks via gradient-based localization," in *ICCV*, pp. 618–626, 2017.
- [21] B. N. Patro, M. Lunayach, S. Patel, and V. P. Nambodiri, "U-cam: Visual explanation using uncertainty based class activation maps," in *ICCV*, pp. 7444–7453, 2019.
- [22] A. Das, H. Agrawal, L. Zitnick, D. Parikh, and D. Batra, "Human attention in visual question answering: Do humans and deep networks look at the same regions?," *CVIU*, vol. 163, pp. 90–100, 2017.
- [23] D. H. Park, L. A. Hendricks, Z. Akata, A. Rohrbach, B. Schiele, T. Darrell, and M. Rohrbach, "Multimodal explanations: Justifying decisions and pointing to the evidence," in *CVPR*, pp. 8779–8788, 2018.
- [24] J. Wu and R. J. Mooney, "Faithful multimodal explanation for visual question answering," in *BlackboxNLP@ACL*, pp. 103–112, 2019.
- [25] W. Yu, J. Zhou, W. Yu, X. Liang, and N. Xiao, "Heterogeneous graph learning for visual commonsense reasoning," in *NeurIPS*, pp. 2765–2775, 2019.

- [26] J. Lin, U. Jain, and A. G. Schwing, "TAB-VCR: tags and attributes based VCR baselines," in *NeurIPS*, pp. 15589–15602, 2019.
- [27] Y. Chen, L. Li, L. Yu, A. E. Kholy, F. Ahmed, Z. Gan, Y. Cheng, and J. Liu, "UNITER: universal image-text representation learning," in *ECCV*, pp. 104–120, 2020.
- [28] W. Su, X. Zhu, Y. Cao, B. Li, L. Lu, F. Wei, and J. Dai, "VL-BERT: pre-training of generic visual-linguistic representations," in *ICLR*, 2020.
- [29] P. Sharma, N. Ding, S. Goodman, and R. Soiccut, "Conceptual captions: A cleaned, hypertexted, image alt-text dataset for automatic image captioning," in *ACL*, pp. 2556–2565, 2018.
- [30] G. E. Hinton, O. Vinyals, and J. Dean, "Distilling the knowledge in a neural network," *CoRR*, vol. abs/1503.02531, 2015.
- [31] Y. Shang, B. Duan, Z. Zong, L. Nie, and Y. Yan, "Lipschitz continuity guided knowledge distillation," in *ICCV*, pp. 10675–10684, 2021.
- [32] J. Ba and R. Caruana, "Do deep nets really need to be deep?," in *NeurIPS*, pp. 2654–2662, 2014.
- [33] P. Liu, W. Liu, H. Ma, Z. Jiang, and M. Seok, "KTAN: knowledge transfer adversarial network," in *IJCNN*, pp. 1–7, 2020.
- [34] Z. Shen, Z. He, and X. Xue, "MEAL: multi-model ensemble via adversarial learning," in *AAAI*, pp. 4886–4893, 2019.
- [35] A. Romero, N. Ballas, S. E. Kahou, A. Chassang, C. Gatta, and Y. Bengio, "Fitnets: Hints for thin deep nets," in *ICLR*, 2015.
- [36] S. Zagoruyko and N. Komodakis, "Paying more attention to attention: Improving the performance of convolutional neural networks via attention transfer," in *ICLR*, 2017.
- [37] X. Jin, B. Peng, Y. Wu, Y. Liu, J. Liu, D. Liang, J. Yan, and X. Hu, "Knowledge distillation via route constrained optimization," in *CVPR*, pp. 1345–1354, 2019.
- [38] J. Yim, D. Joo, J. Bae, and J. Kim, "A gift from knowledge distillation: Fast optimization, network minimization and transfer learning," in *CVPR*, pp. 7130–7138, 2017.
- [39] K. He, G. Gkioxari, P. Dollár, and R. Girshick, "Mask r-cnn," in *ICCV*, pp. 2961–2969, 2017.
- [40] K. He, X. Zhang, S. Ren, and J. Sun, "Deep residual learning for image recognition," in *CVPR*, pp. 770–778, 2016.
- [41] J. Devlin, M.-W. Chang, K. Lee, and K. Toutanova, "Bert: Pre-training of deep bidirectional transformers for language understanding," *arXiv preprint arXiv:1810.04805*, 2018.
- [42] A. Jabri, A. Joulin, and L. Van Der Maaten, "Revisiting visual question answering baselines," in *ECCV*, pp. 727–739, Springer, 2016.
- [43] P. Anderson, X. He, C. Buehler, D. Teney, M. Johnson, S. Gould, and L. Zhang, "Bottom-up and top-down attention for image captioning and visual question answering," in *CVPR*, pp. 6077–6086, 2018.
- [44] J.-H. Kim, K.-W. On, W. Lim, J. Kim, J.-W. Ha, and B.-T. Zhang, "Hadamard product for low-rank bilinear pooling," in *ICLR*, 2017.
- [45] H. Ben-Younes, R. Cadene, M. Cord, and N. Thome, "Mutan: Multi-modal tucker fusion for visual question answering," in *ICCV*, pp. 2612–2620, 2017.



Zhenyang Li received the B.Eng. and master degree from Shandong University and University of Chinese Academy of Sciences, respectively. He is currently pursuing the Ph.D. degree with the School of Computer Science and Technology, Shandong University, supervised by Prof. Liqiang Nie. His research interest is multi-modal computing, especially visual question answering.



Yangyang Guo is currently a research fellow with the National University of Singapore. He has published several papers in top conferences and journals such as IEEE TIP, IEEE TMM, IEEE TKDE and ACM TOIS. He has served as a Regular Reviewer for journals, including IEEE TMM, IEEE TKDE, ACM TOIS, ACM ToMM.



Kejie Wang is currently pursuing the B.Eng. degree in computer science from the Shandong University. His research interests include visual question answering and computer vision.



Yinwei Wei (Member, IEEE) received his MS degree from Tianjin University and Ph.D. degree from Shandong University, respectively. Currently, he is a research fellow with NExT, National University of Singapore. His research interests include multimedia computing and recommendation. Several works have been published in top forums, such as ACM MM, IEEE TMM and TIP. Dr. Wei has served as the PC member for several conferences, such as MM, AAAI, and IJCAI, and the reviewer for TPAMI, TIP, and TMM.



Liqiang Nie (Senior Member, IEEE) is currently a professor with Shandong University and the dean with the Shandong AI institute. He received his B.Eng. and Ph.D. degree from Xi'an Jiaotong University and National University of Singapore (NUS), respectively. After PhD, Dr. Nie continued his research in NUS as a research fellow for three years. His research interests lie primarily in multimedia computing and information retrieval. Dr. Nie has co-authored more than 100 papers and 4 books, received more than 13,000 Google Scholar citations.

He is an AE of IEEE TKDE, IEEE TMM, IEEE TCSVT, ACM ToMM, and Information Science. Meanwhile, he is an area chair of ACM MM 2018–2022. He has received many awards, like ACM MM and SIGIR best paper honorable mention in 2019, SIGMM rising star in 2020, TR35 China 2020, DAMO Academy Young Fellow in 2020, and SIGIR best student paper in 2021.



Mohan Kankanhalli (Fellow, IEEE) received the B.Tech. degree from IIT Kharagpur and the M.S. and Ph.D. degrees from Rensselaer Polytechnic Institute. He is currently the Provost's Chair Professor with the Department of Computer Science, National University of Singapore (NUS). He is also the Director of N-CRIPT and the Dean of the School of Computing, NUS. His current research interests are in multimedia computing, multimedia security and privacy, image/video processing, and social media analysis. He is on the editorial boards of several

journals.